

# Qubit operations using a modular optical system engineered with PyOpticL: a code-to-CAD optical layout tool

Jacob Myers,<sup>1</sup> Christopher Caron,<sup>1</sup> Nishat Helaly,<sup>1</sup> Zhenyu Wei,<sup>1</sup> Justin Oh,<sup>1</sup> Zack Gotobed,<sup>1</sup> Kotaro Yabe,<sup>1</sup> and Robert J. Niffenegger<sup>1,\*</sup>

<sup>1</sup>*University of Massachusetts Amherst, Dept. Electrical and Computer Engineering, Amherst, MA*  
(Dated: January 28, 2025)

Complex optical design is hindered by conventional piecewise setup, which prevents modularization and therefore abstraction of subsystems at the circuit level. This limits multiple fields that require complex optics systems, including quantum computing with atoms and trapped ions, because their optical systems are not scalable. We present an open-source Python library for optical layout (PyOpticL) which uses beam-path simulation and dynamic beam-path routing for quick and easy optical layout by placing optical elements along the beam path without a priori specification, enabling dynamic layouts with automatic routing and connectivity. We use PyOpticL to create modular ‘drop-in’ optical baseplates for common optical subsystems used in atomic and molecular optics (AMO) experiments including laser sources, frequency and intensity modulation, and locking to an atomic reference for stabilization. We demonstrate this minimal working example of a dynamic full laser system for strontium trapped ions by using it for laser cooling, qubit state detection, and 99.9% fidelity single-qubit gates with 3D printed baseplates. This enables a new paradigm of design abstraction layers for engineering optical systems leveraging modular baseplates, as they can be used for any wavelength in the system and enables scaling up the underlying optical systems for quantum computers. This new open-source hardware and software code-to-CAD library seeks to foster open-source collaborative hardware and systems design across numerous fields of research including AMO physics and quantum computing with neutral atoms and trapped ions.

## INTRODUCTION

Careful optical design is critical for high-performance, stable and compact optical layouts for atomic and molecular optical (AMO) physics based experiments for fundamental physics and sensing applications, as well as for quantum computers based on neutral atoms and trapped ions. Miniaturizing layouts to optical baseplates [1, 2] and micro-optics [3–5] improves stability and performance, while simultaneously enabling rack mounting and portable operation. However, neither miniature baseplates nor micro-optics are widely used due to the difficulty of customizing and updating their designs using existing 3D CAD tools.

For electronics and VLSI design, tools like Cadence are critical enablers, which dynamically manage layouts while automatically routing connections between components. VLSI design tools also utilize hierarchical abstraction of levels so that the functional level of design is not burdened by the device level.

In photonics, open source tools for layout like GDSFactory [6] have created an open source collaborative community that dramatically lowers the barrier to entry for advanced and large-scale photonic layout. Despite the advantages of using CAD for optical circuit design, there is no tool that can dynamically position optical elements and route connections simultaneously. This means that optical circuit design can not abstract away these aspects of design at the device level (optical element), preventing the abstraction to higher levels of the optical system hierarchy and therefore scalable optical systems engineering.

Here we present and demonstrate an open-source Python tool for optical layout, called ‘PyOpticL’[7] (<https://github.com/UMassIonTrappers/PyOpticL>).

This optical layout library is built on another open source software tool, FreeCAD [8], which is also based on Python, making them seamlessly compatible and easily expandable.

Building on top of another open source tool itself, PyOpticL seeks to emulate and complement other open source hardware movements in the AMO and quantum computing community, such as ARTIQ (M-Labs) [9], which has created a central open source hardware development hub for the precise electronic control hardware required for precision AMO and quantum computing experiments. This enables collaborative hardware projects which can be developed and maintained by a large and growing community of researchers.

Critically, the modularization of several optical circuits for modulation and stabilization enables abstraction of these levels within the larger AMO apparatus, as these same optical baseplates can be applied to all of the wavelength-specific subsystems.

Additionally, the script-based nature of the optical layouts designed in PyOpticL enables the hardware design process to be managed via version control similar to software development, enabling easy publishing of hardware designs and collaborative convergence on best-known methods across disciplines.

## PYOPTICL

### Ad Hoc Piecewise optics

Piecewise placement and alignment of optical elements is a tedious and slow process. This burden prohibitively restricts how frequently optical layouts are updated or revised, as it is often not possible to revise the position or angle of any single optical element without perturbing the entire downstream optical beam path.

While it is possible to isolate optical degrees of freedom of optical path branches, through the use of polarizing beam-splitters (PBS) etc., this still does not often translate into a modular layout, due to the underlying monolithic nature of mounting all individual optical elements piecewise to a single optical table.

Smaller optical breadboards offer a way to modularize optical subsystems, but in practice are seldom utilized for this purpose. Even on a breadboard, the subsystems are often too large to be modular, and these breadboards themselves must be still manually aligned, one optical element at a time, to a fixed grid.

Smaller half-inch optics have been used to build compact optical systems for AMO applications such as trapped ions [10–13]. However, they are often still set up ad hoc upon a fixed grid similar to an optical table, such that precise, serial placement and alignment of all optical elements is still required.

To overcome these challenges, there have been many “in-house” [2, 10, 14] and also proprietary [15, 16] solutions to optical layout using 3D CAD software like SolidWorks, which allow users to precisely place optical elements and define a custom baseplate to mount them. This dramatically aids in the precise positioning and angular alignment during the placement of optical elements upon the baseplate, making optical setup as easy as ‘paint by numbers’.

This drop-in alignment is especially critical for micro-optics [3] which use 3 mm optical elements and are placed without any adjustable mounts, preventing re-alignment after elements are placed.

However, these designs are all static and there is no way to dynamically update the optical elements in the circuit nor the layout of the circuit, which must be tweaked/aligned manually within the CAD software. This means that substantial alignment time is still required *within* the CAD environment, eroding the time-saving benefits of pre-designing the layout. This also means that changing any single optical element in the design (or converting from 1/2-inch to micro optics) requires a total re-alignment of the layout within the CAD environment, limiting how broadly the static designs can be applied for various wavelengths etc. Even parameterizing the layout eventually becomes manual without beam tracking. Additionally, this beam alignment veri-

```

1 # define and place baseplate object
baseplate = layout.baseplate(base_dx, base_dy, base_dz)

# add beam
beam = baseplate.add_beam_path(x=gap, y=input_y, angle=layout.cardinal['right'])

3 # add waveplate along the transmitted beam, 25 mm from the beam input
baseplate.place_element_along_beam("Rotation Stage", optomech.waveplate, beam,
                                   beam_index=0b1, distance=25,
                                   angle=layout.cardinal['right'],
                                   mount_type=optomech.rotation_stage_rsp05)

4 # add cube splitter component along beam, 30 mm from the waveplate
baseplate.place_element_along_beam("Beam Splitter Cube", optomech.cube_splitter, beam,
                                   beam_index=0b1, distance=30,
                                   angle=layout.cardinal['right'],
                                   mount_type=optomech.skate_mount)

5 # add mirror along the reflected beam, 1 inch from the splitter cube
baseplate.place_element_along_beam("Mirror", optomech.circular_mirror, beam,
                                   beam_index=0b11, distance=layout.inch,
                                   angle=layout.turn['up-right'],
                                   mount_type=optomech.mirror_mount_k05s1)

```

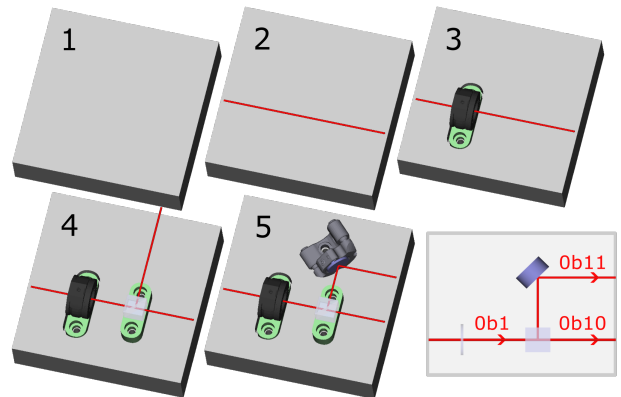


FIG. 1. **Code-to-CAD system:** An example of how a simple baseplate can be scripted using along-beam placement.

fication process is manual, as there is no ability within these CAD tools to track beam paths and verify beam alignment between optical elements.

### Dynamic optical routing

Many of these issues stem from the lack of dynamic routing of the optical layout. All CAD software used for electronic and photonic circuit layout has some form of dynamic routing which aids in adjusting the layout without breaking connectivity within the circuit. Here, we present a new architecture for optical layout based on our custom Python library (PyOpticL) which uses ‘beam-based routing’, to automatically track the optical beam-path throughout the circuit and place optical elements *along* the laser beam’s path, as defined by a simple script. We also define a set of simple design rules (see SI for details) which enable a modular and scalable design for interchangeable parts within a complex optical system.

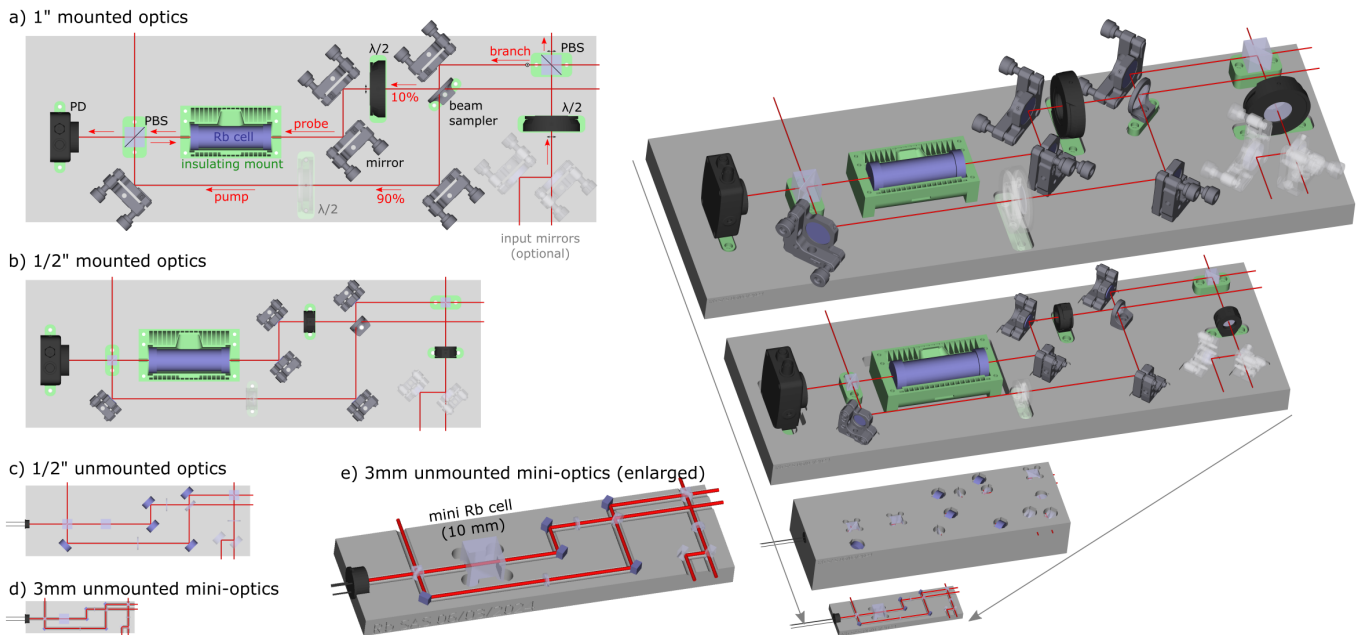


FIG. 2. **Dynamic Layout to micro-optics:** The same base optical layout code can be arbitrarily recompiled with different components for each optical element and at different scales. As an example, the same Saturated Absorption Spectroscopy layout script can be compiled at 4 different scales with 4 different sets of optics: (a) 1 inch optics, (b) 1/2 inch mounted optics, (c) ‘mount-free’ 1/2 inch optics, (d) 3 mm micro-optics. The underlying layout is identical for all layouts, but the dictionaries called for the individual optical elements and relative distances are different in each baseplate, demonstrating the dynamic possibilities of code based CAD layout.

### FreeCAD vs. OpenSCAD

The underlying CAD software upon which to build the PyOpticL library is critical. Two popular open-source options are FreeCAD [8, 17] and OpenSCAD [18]. OpenSCAD relies on a scripted design with minimal graphical user interface, which is well suited for parameterized design. OpenSCAD also uses an entirely mesh-based object system, optimal for 3D printing<sup>1</sup>. However, OpenSCAD’s scripting language is not capable of dynamic beam path routing, because variables cannot be modified at runtime (e.g.  $x = x + 1$  is not possible) [19]. In addition, OpenSCAD’s rendering slows dramatically with model complexity, requiring minutes to render layouts with more than a few optical elements. This makes the design phase prohibitively slow as each iteration to update the code and re-render can take minutes.

FreeCAD [8, 17] is more flexible and provides both a fully featured graphical user interface and a Python-based scripting back-end. The Python back-end allows FreeCAD to be easily tailored for specialized applications through community-built add-ons, called workbenches.

<sup>1</sup> We wish to note that the MIT Quanta lab led by Professor Chuang has developed a library for optical layout based on OpenSCAD and that they have graciously shared this library with us prior to the development of PyOpticL.

They add both scripting and GUI based functionality through importable Python modules. FreeCAD also supports dynamic variables at runtime and renders parametric models quickly, enabling dynamic layout and rapid iterations during design.

### Beam Simulation

In order to facilitate accurate modeling and dynamic routing for layout, a robust beam simulation system is required. PyOpticL uses a simplified beam-tracing system which relies on a set of defined rules for different optical components. Optical parameters for reflection, transmission, focal length, and diffraction angle allow modeling of a wide range of optics such as mirrors, splitters, lenses, and gratings. Relying on a path-based system rather than a ray-traced approach not only reduces the computational load significantly but also greatly improves the ease of importing models through the simple parameterization of optical properties. Sophisticated 3D ray tracing is in development, and we have used it to design larger 3D optical systems (Fig. 7).

Beams are defined with an initial position and global orientation representing the incoming beam or source. For simplicity, we follow a convention that these paths stay along the cardinal directions of the underlying optical table grid. Using the initial beam definition, the

## PyOpticL Design Abstraction Layers

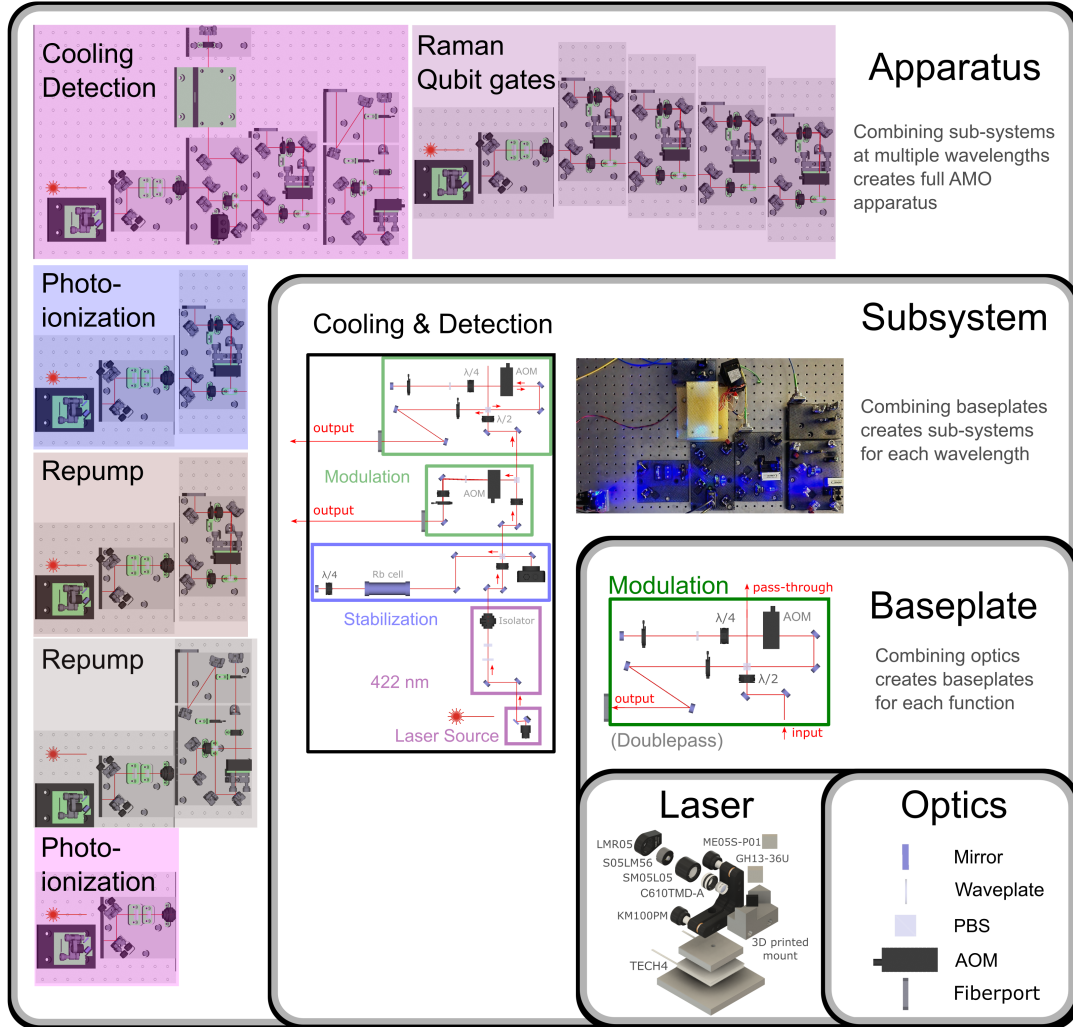


FIG. 3. **Hierarchical layers of design abstraction that are enabled by PyOpticL applied to a strontium trapped ion quantum computer:** Standard, commercially available optical elements are the foundational abstraction layer of the optical system. Higher level designs can use variables or dictionaries to define optical elements with which to compile baseplates or subsystems. Where each optical element can have predefined characteristic distances and properties dynamically determining the final compiled optical layout. Next, some optics assemblies are stand-alone but not baseplates, such as the extended cavity diode laser (ECDL). Next, baseplates combine individual optical elements for specific functions, such as intensity and frequency modulation with AOMs. To be abstractable, baseplates must be modular and fit within any larger optical sub-system with minimal customization. This means their input and output beams must conform to design rules so that all beams enter and exit along the grid of the optical table and flow in the same direction between baseplates. Next, combining baseplates for various functions creates self contained subsystems at each wavelength, encompassing even the laser source. Lastly, combining multiple subsystems at multiple wavelengths (all utilizing the same underlying baseplate designs for modulation and laser sources etc.) creates an entire apparatus. In this case, a strontium trapped ion quantum computer.

system will calculate subsequent optical interactions as defined in the component library. This complete automation of beam path modeling both saves time during layout design and improves the ease and confidence with which layout issues such as collisions or misalignment can be detected and resolved.

### Dynamic layout along beam path

The ability to sequentially predict the path of the beam as it interacts with optical elements allows a new paradigm of optical layout which sets new optics along the path of the beam dynamically, without using any fixed coordinates within the CAD system. To do this,



an object’s position is defined by the beam on which it will be placed, the sub-beam index, and an additional constraint such as a distance from the last component or a single absolute x or y coordinate. The sub-beam index here refers to the way in which the beam path is segmented in the case of splits or diffraction. In order to facilitate placement along any arbitrarily branching path, a non-repeating beam indexing system is required. For this case, a binary tree system was used (Fig. 1). The initial beam is given index one, or ‘0b1’ as a binary literal. When the beam passes through a splitter, a zero or one is appended to the binary index of the transmitted (0) and reflected (1) beams respectively. So in the case of the first split in a path, the transmitted beam would have index ‘0b10’ and the reflected beam would have index ‘0b11’. In this way, not only are the beam indexes unique for any arbitrary path, but they remain highly readable due to the direct correlation to the binary literal and the path taken to arrive at that beam segment.

### CODE-TO-CAD: DYNAMIC LAYOUT AND ROUTING

PyOpticL leverages this dynamic beam path routing to create an intuitive and efficient code-to-CAD optical layout tool, allowing for dynamic and easily modified optical layouts. Components can be defined via coordinates on the baseplate, relative to the beam path, or relative to other components. Using these varying placement methods, it is easy to create layouts which are entirely constrained to the beam path. This method of design allows for the entire layout to dynamically adjust whenever a single element is moved or modified, and therefore automatically preserves the desired beam path and maintains connectivity. This means that many subtle adjustments can be made through the course of rapid development within the CAD environment without ruining the entire layout.

A choice to use a global set of beam directions allows mounts to be placed so that they accept one orientation of beam input and output another (e.g. ‘up-right’ accepts a beam going ‘up’ and turns it ‘right’). These orientations are not relative to the beam path, meaning that “up/down” and “left/right” are defined globally with respect to the baseplate. This means that no angles are needed to script the layout. (We note that arbitrary angles are possible and certainly beneficial in particular instances like very compact layouts.)

The scripted nature of the library also allows for highly parameterized designs through the use of local variables. For instance, the type of mirror used throughout an entire layout could be easily changed simply by defining it as an argument or a variable in that layout’s script. Furthermore, components can be dynamically designed

to adapt to varying parameters, such as adapter plates generated on-demand for different mounting angles based on application-specific wavelengths or optical properties like grating pitch.

Code-to-CAD design therefore enables layouts to be recompiled with entirely different sets of mounts, or indeed, no mounts at all, if a full monolithic mounting is desired. To demonstrate this capability, we recompile the same saturated absorption spectroscopy (SAS) layout in four cases: 1. 1-inch mounted optics, 2. 1/2-inch mounted optics, 3. 1/2-inch unmounted optics, 4. Mini-optics, shown in Figure. 2. A dictionary serves as the look-up table for which mirror or lens is required, and the relative distance scaling, without any modification of the layout. We note that there are *many* examples of small SAS setups [4, 20–24], but they are static designs.

### Importing new optical components

One critical bottleneck in a code-to-CAD system can be the introduction of new components into the library. It is critical that adding new mounts (even new custom designs) is streamlined and precise. Otherwise, the time to align the CAD model to these mounts can return to a tedious trial-and-error process, which defeats the purpose of the system entirely. Therefore, we have developed and tested a rapid import procedure within FreeCAD that quickly sets the center of the mounts and their base positions to easily import them to the library and layout (see SI and GitHub [7] for details). It is also possible to import non-optical elements like vacuum chambers, etc. to register beam delivery to an experimental apparatus.

### Optical subsystems for AMO and quantum computing experiments

There are a few key subsystems for optics within all atomic and molecular optical physics experiments, including quantum computing with neutral atoms and trapped ions.

1. **Laser** - Extended cavity diode lasers (ECDLs) as a source of narrow linewidth laser light.
2. **Laser stabilization** - Locking to atomic transitions for absolute laser stabilization.
3. **Pulse control** - Acousto-optical modulators for modulating the laser intensity and frequency. Commonly with ‘single-pass’ and ‘double-pass’ configurations.
4. **Beam delivery** - Finally, the light must be delivered to the target trapped ion, atom, sample, etc., with a precisely aligned lens.

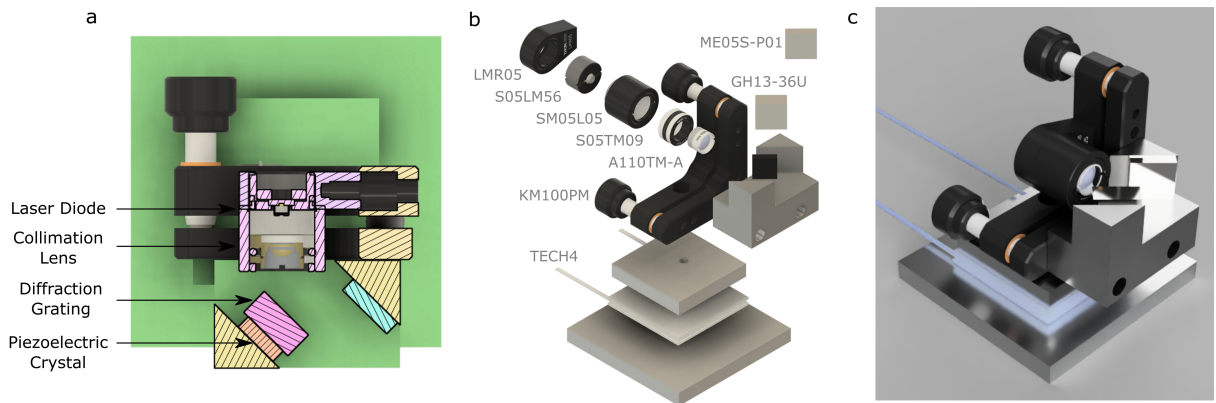


FIG. 4. **Extended cavity diode laser:** PyOpticL 422 nm extended Cavity Diode Laser (ECDL) with almost all off-the-shelf components. The only custom part is a 3D printed mount for the grating with a dynamic Littrow angle.

Here we outline the development of example or template baseplates for each of these applications, which are readily reconfigurable for any wavelength and numerous AMO applications, using the PyOpticL library (Figure 3). The full setup can be created by importing each baseplate as a function, matching their input and outputs manually relative to the underlying 1-inch grid of the optical table (a much easier task than aligning each optical element individually). We have found that in practice further automatic alignment is not necessary.

```

1 from PyOpticL import layout, optomech
2 from ECDL import ECDL
3 from Rb_SAS.V2 import Rb_SAS
4 from modular_doublepass import doublepass
5 from modular_singlepass import singlepass
6
7 def laser_cooling_subsystem():
8     layout.table_grid(dx=36, dy=22)
9     ECDL(x=27, y=20, angle=180)
10    Rb_SAS(x=20, y=1, angle=90)
11    singlepass(x=14, y=12, angle=90)
12    doublepass(x=1, y=21, angle=270)

```

### Dynamic Extended Cavity Diode Laser (ECDL)

Homemade extended cavity diode lasers at near-IR wavelengths were an enabling tool for pioneering AMO laboratories [25], which needed many narrow linewidth lasers for various atomic transitions and operations such as laser cooling and repumping. However, these designs are all static and require the machining of multiple custom components [22, 25–32].

Here we focus on designing an extremely simple ECDL with only a single custom part, a dynamic 3D printed mount for the diffraction grating, generated in PyOpticL. All other parts are off-the-shelf with no modification or machining at all. The 3D printed grating mount attaches directly to the ubiquitous KM100PM Thorlabs mount without modification. As an example, we demonstrate

laser operations at 421.6 nm, which is useful for strontium trapped ions and also neutral rubidium for Rydberg applications.

We mount a 418 nm laser diode (TopGaN, no AR coating) within a 1/2 inch lens tube (SM05L05), threaded to the front of the LMR05, which is directly mounted to a KM100PM (Figure 4). The KM100PM is mounted onto a small aluminum block, which is hand cut from 1/4 inch stock with a single drilled and 8-32 threaded hole. A TEC (TECH4) is then sandwiched with another aluminum block and controlled by a TED200C (see SI for more details).

The feedback for the extended cavity diode laser is provided by a diffraction grating (GH13-36U, 7% at 421nm) mounted on a parameterized custom 3D printed mount generated by PyOpticL. The Littrow angle of the grating is set by the wavelength and the diffraction grating pitch, allowing the mount design to be dynamically reconfigured for arbitrary wavelengths. We have simplified this design to minimize the amount of machining required. This mount can be milled from aluminum with a single set angle of milling and drilling two holes (with counter-sink). We note that the 3D printed mount shows remarkable stability and was used for all experiments.

We tuned the laser diode free-running wavelength of 418.9 nm up to 421.6 nm (-4.6 THz) by heating it to 50 C. Thermally isolating the laser within a 3D printed box enabled stability within 100MHz for hours measured by a MOGLabs Fizeau wavemeter and verified with saturated absorption spectroscopy.

To further isolate and stabilize the laser we created a totally enclosed 3D printed box with a port for a Brewster window for light to exit. This dramatically improved the laser stability over the ‘open-to-air’ box (see SI Figure 8), reducing drift from 2MHz/s to 30kHz/s and reducing fast frequency noise.

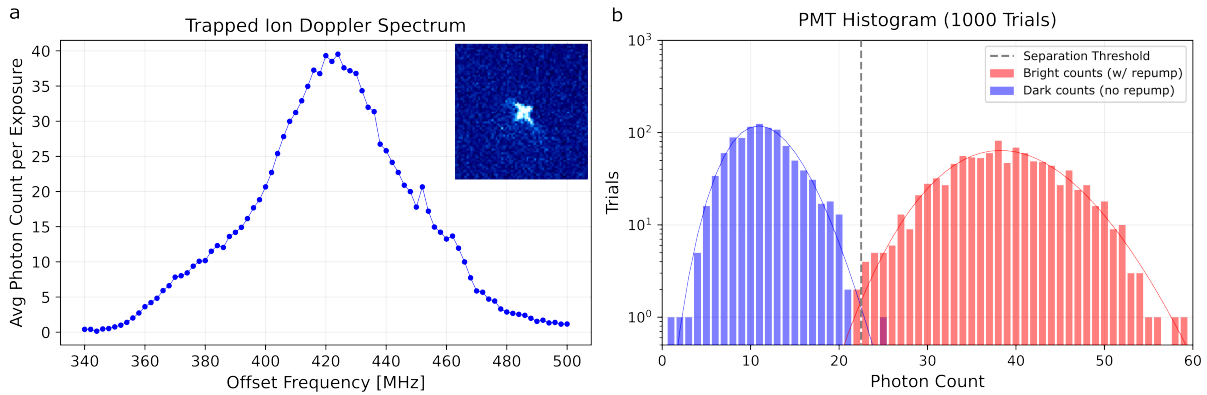


FIG. 5. **Trapped ion laser cooling and detection:** a) Doppler scan of the brightness of the trapped ion while scanning the frequency of the double-pass AOM sending light to the ion from the custom 422 nm ECDL locked to the Rb SAS (Inset: Trapped ion, cooled and detected with custom ECDL). b) Detection histogram of the trapped ion using the custom 422 nm ECDL shows high fidelity detection (99.8%) in 2 ms detection time. Dark counts are measured by manually blocking the repump laser (1092 nm).

### Laser stabilization with Saturated Absorption Spectroscopy

To demonstrate stable single-mode operation of the ECDL we use it to observe saturated absorption spectroscopy (SAS). SAS is commonly used to lock and stabilize lasers using an atomic transition. We note that *many* other examples of small SAS setups exist [3, 22–24] and are commercially available [20, 33].

Here we create saturated absorption spectroscopy (SAS) layouts using PyOpticL (Fig. 2), and build the 1/2 inch mounted optics plate (see SI for more details). Tuning the laser to the resonance of rubidium enabled capture of Doppler-free peaks (SI Figure 9a).

Next, we stabilize the ECDL frequency by locking to the  $s^2S_{1/2} \rightarrow 6p^2P_{1/2}$  transitions  $^{85}\text{Rb}$  ( $F = 2 \rightarrow 2,3$ ) [34, 35] using the open-source software Linien [36] and a Red Pitaya. Locking feedback was applied through the voltage to the PZT, and modulation was added via the Thorlabs current controller. We observed that the lock was stable for hours at a time over the course of weeks.

### Laser cooling and detection

With the ECDL locked to the rubidium ( $F = 2 \rightarrow 2,3$ ) transition by the SAS baseplate, we then used the double-pass AOM baseplate to control the laser intensity and frequency, spanning the gap to resonance with the strontium ion ( $5S_{1/2} \rightarrow 5P_{1/2}$  transition) for Doppler cooling and detection [34, 35, 37].

We used this complete PyOpticL optical subsystem to laser-cool trapped  $^{88}\text{Sr}^+$  ions (Figure 5a, inset) for hours at a time over the course of weeks. To verify precise frequency control via the double-pass AOM baseplate we also measure the brightness of the ion while scanning

across resonance, measuring the Doppler curve of the trapped ion (Figure 5a). This also verifies that the SAS lock baseplate stabilized the laser to within a few MHz. Finally, we verified that the system can perform high-fidelity state detection (Figure 5b), measuring 99.8% fidelity with a detection time of 2 ms. The dark counts are measured by manually blocking a repump laser.

### Raman Laser for Zeeman qubit gate operations

Using the same ECDL design and a different 422 nm diode (Nichia) we built a Raman laser for Zeeman qubit gate operations between the spin sublevels of the ground state (Fig. 6a). We used the single-pass AOM baseplates to create two tones ( $\omega_1, \omega_2$ ) with independent intensity and frequency control and combined them into the same optical fiber for co-propagating delivery to the ion. To create a Zeeman qubit [38], we then set the difference of the two tones equal to the frequency of the Zeeman splitting between the sublevels ( $\delta = \omega_Z - (\omega_1 - \omega_2) = 0$ ) and pulsed the Raman beams to excite spin transitions of the ground state (Fig. 6b). To test qubit operations, we tuned the Raman laser 200 GHz from resonance (to reduce the error from spontaneous emission [39] to below 0.1%) and were able to measure Raman Rabi oscillations (Fig. 6c), with single-qubit gate fidelity of 99.9%. We measure magnetic field noise limited coherence times of 550  $\mu\text{s}$  which can be increased to 3.4 ms by triggering experiments to the AC mains. In the future, adding Mu-metal shielding could extend it beyond a second [38].

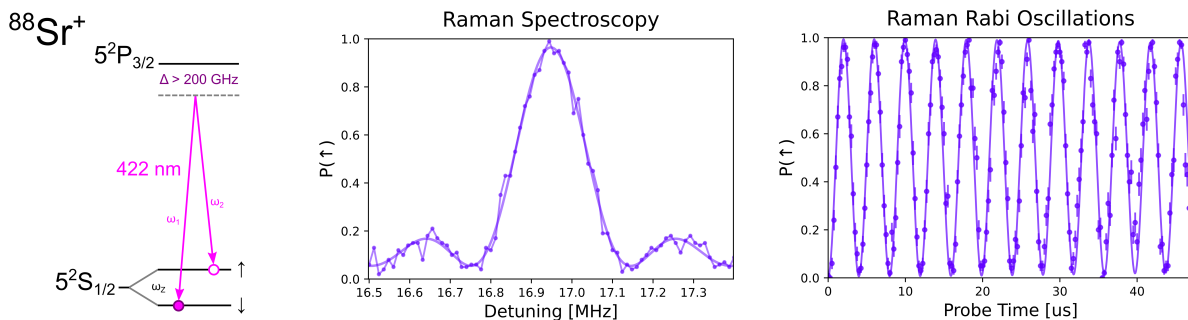


FIG. 6. **Zeeman qubit operations with Raman laser:** a) Sublevels of the ground state of  $^{88}\text{Sr}^+$  are Zeeman split by  $\omega_Z$  from an applied 6 Gauss magnetic field. The Raman beams are detuned by  $\Delta > 200$  GHz from the excited state, and their relative frequency is set to resonance with the splitting of the ground state. b) Raman resonance when  $\delta = \omega_Z - (\omega_1 - \omega_2) = 0$ , shows the Zeeman splitting is  $\omega_Z = 2\pi \cdot 16.95$  MHz. c) Raman Rabi oscillations show a single qubit gate fidelity of 99.9%.

### Dynamic Laser System Demonstration

Altogether, we have demonstrated a fully dynamic AMO apparatus (Figure 3) with modular optical subsystems that are dynamically reconfigurable for innumerable AMO applications, including quantum computing with trapped ions and neutral atoms. Each optical subsystem can be recompiled for any wavelength and, therefore, any atomic species. This means that nearly identical subsystems to those we have demonstrated could be used for a neutral-atom AMO apparatus. For example, a Bose-Einstein condensate apparatus [40, 41] could use the same cooling and detection subsystem layouts that we have demonstrated but with optics for 780 nm, and a duplicate subsystem could perform repumping. Even more directly, the exact same laser cooling subsystem that we have demonstrated could be used in a neutral-atom quantum computer based on Rb [42] as they also require lasers at 421 nm and lock to Rb for stabilization.

This modularization and standardization of optical circuits begins to enable design abstraction methods similar to those used in digital logic systems. Where details of the underlying optical baseplate are abstracted away, with only their function in the optical system being important for design. This paradigm is critical not only for rapid and sustainable development, but also for scaling. VLSI would not scale without abstraction or without modularization and standardization of the underlying subsystems.

### RAPID PROTOTYPING WITH 3D PRINTING

Over the course of this project prototypes of optical baseplates were printed using an Elegoo Saturn 3D resin printer, with engineering resin (or high-temperature resin for the heated vapor cell holder). New baseplates layouts can be rapidly prototyped with 3D printing, then swapped with the old baseplate to verify placement of

all optics before machining a metal version. The modular nature of the baseplates with respect to each other makes them very easy to swap and re-organize as needed without realigning their constituent optical elements.

All baseplates are designed to be easily CNC milled out of aluminum to maintain the stability of the underlying commercial optical mounts and maximize the stability of the full layout. This means that all designs use a subtractive drilling operation within PyOpticL so that baseplates can be easily machined from 1 inch thick stock aluminum. PyOpticL automatically generates technical CAD drawings of the designs, including annotations noting threaded holes etc. to streamline ordering and machining.

In practice, we found that the 3D printed baseplate prototypes made with engineering resin (which can be threaded) worked better than anticipated, depending on the application. We have observed that smaller 3D printed baseplates with a higher density of mount points to the optical table perform the best and have stability similar to our traditional optics and do not require frequent realignment. We believe this is because they conform to the underlying optical table the best and inherit the stability of the optical table better. The exception was periscopes, which due to their height required the input optical path to be farther from the plane of the optical table, making them especially susceptible to warping and deformation, such that they could not remain aligned for more than a day. 3D printing a periscope with a broad base improved stability, but was not sufficient. Still, periscopes were the only element where an aluminum version was absolutely necessary and most flat 3D printed baseplates worked well.

For mounting individual optics like PBS and rotation mounts, small 3D printed fixed adapters may be sufficient without aluminum machining, as their small size limits their deformation.

It is interesting to note that for some applications, 3D printing a ‘mount free’ baseplate without any commer-



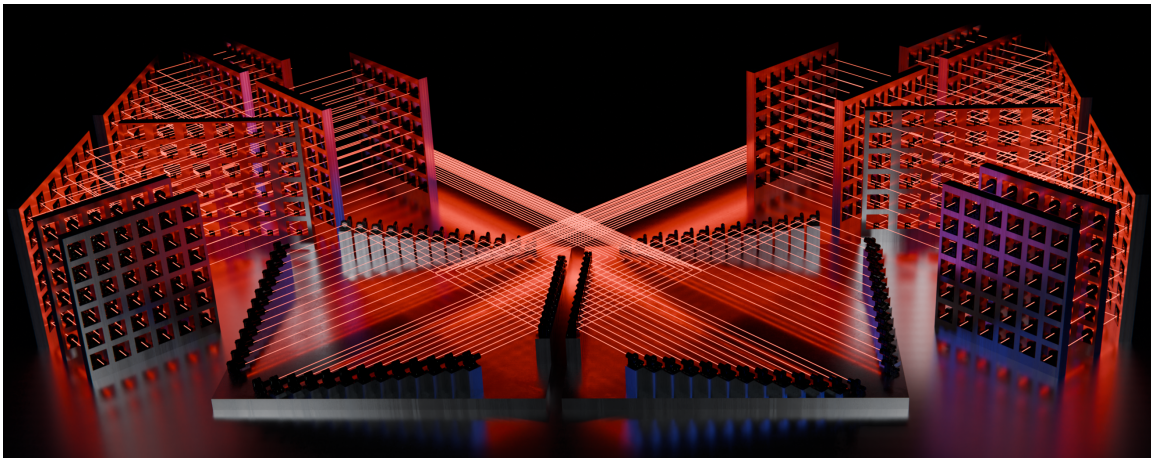


FIG. 7. **Scalable optical layout:** To showcase the scalable nature of the code-to-CAD design paradigm we roughly recreate the optical layout used in a recent optical interferometry experiment [43]; using for-loops to layout the individual optical elements in grid mounts tracking the laser beam for each path. We then render the CAD model in Blender.

cial adjustable mounts could be sufficient and much more compact (Fig. 2c), dramatically lowering the cost for these optical systems and making them more accessible for broader educational applications.

While we anticipate the future development of 3D printed adjustable mounts within the PyOpticL library to replace the commercial adjustable mounts, we are cautious that the compromise in performance with entirely 3D printed adjustable mounts for most applications would be unjustifiable.

## SCALABLE OPTICAL DESIGN

Script-based optical design enables new paradigms of scalable optical layout through inheritance of the scalable nature of code. To showcase this, we used PyOpticL to roughly recreate the layout (Figure 7) from an optical interferometry experiment [43] designed to demonstrate quantum supremacy through Boson Sampling. The experiment used custom vertical arrays ( $6 \times 6$ ) of optical elements and input layouts of sets of 50 optical elements. We hope that this example inspires more creative applications of PyOpticL with sophisticated 3D routing between modular baseplates.

We also note that this scaling is critical for the broader adoption of micro-optics, which are more practically capable of creating such large optical setups.

## DISCUSSION

We hope that PyOpticL becomes a hub for open-source hardware development of optical layouts and optical systems, as more baseplates and layouts are created for new applications. We also hope that this demonstration of

a full laser system comprised of multiple modular subsystems including: laser sources, spectroscopy and stabilization, and modulation baseplates for laser cooling, detection, and qubit gates with trapped ions provides a solid foundation that is already applicable to a broad array of AMO experiments.

Our ECDL design is one fifth of the cost of commercial lasers, delivers twice the power, and can be assembled with off-the-shelf components (except for a single 3D printed part) in minutes after next-day shipping from Thorlabs, dramatically lowering the barrier to entry into AMO and quantum computing for education and research. Total costs for our ECDL are \$7k, with almost half of that cost being the relatively expensive 420 nm laser diode itself (\$3k) and most of the rest being the optical isolator and commercial current, temperature and PZT controllers, which could be swapped for homemade designs [29] if reducing cost is paramount. Demonstration of locking to an atomic cell, qubit operations, and high fidelity qubit gates demonstrates that these lasers are more than sufficient for any precision AMO application.

In the future, we also hope to continue to pursue more micro-optic layouts utilizing novel 3D printing techniques with materials that are stable enough for long-term operation. We are also optimistic that more advanced additive manufacturing could enable the integration of the UHV chamber [44] directly into the PyOpticL library, which in turn could enable creative and unconstrained layouts for optical delivery.

We also hope that in conjunction with other open-source projects like M-Labs ARTIQ and Sinara [9] to create a fully open-source quantum computer ecosystem to increase the accessibility of quantum computers.

## AUTHOR CONTRIBUTIONS

R.J.N. conceived of the work. J.M., J.O., and R.J.N. wrote the PyOpticL library. N.H. and Z.W. performed the SAS and trapped ion experiments with assistance from C.C. and R.J.N. The Raman qubit experiments were performed by C.C., Z.W., and N.H. with assistance from R.J.N. All authors contributed to developing optical baseplates using the library. All authors discussed the results and contributed to the writing of the paper. R.J.N. supervised the research.

## ACKNOWLEDGMENTS

This material is based upon work supported by the National Science Foundation under Grant No. (2338369). The authors gratefully acknowledge Professor Isaac Chuang for inspiring this work. He and his team at the MIT Quanta Lab developed an optical layout library within OpenSCAD called CAD for Precision Optics (C4PO) which inspired this work.

---

\* Correspondence email address: [rniffenegger@umass.edu](mailto:rniffenegger@umass.edu)

- [1] S. Kulkarni, A. Umińska, J. Gleason, S. Barke, R. Ferguson, J. Sanjuán, P. Fulda, and G. Mueller, *Applied optics* **59**, 6999 (2020).
- [2] Z. Zhang, J. Xiang, Y. Meng, W. Ren, S. Deng, and D. Lü, *Optical Fiber Technology* **72**, 102974 (2022).
- [3] S. A. Knappe, H. G. Robinson, and L. Hollberg, *Optics express* **15**, 6293 (2007).
- [4] V. Maurice, Z. L. Newman, S. Dickerson, M. Rivers, J. Hsiao, P. Greene, M. Mescher, J. Kitching, M. T. Hummon, and C. Johnson, *Optics Express* **28**, 24708 (2020).
- [5] A. Strangfeld, S. Kanthak, M. Schiemangk, B. Wiegand, A. Wicht, A. Ling, and M. Krutzik, *JOSA B* **38**, 1885 (2021).
- [6] “gdsfactory 7.25.2 — gdsfactory,” <https://gdsfactory.github.io/gdsfactory/index.html>.
- [7] “PyOpticL,” <https://github.com/UMassIonTrappers/PyOpticL>.
- [8] “FreeCAD: Your own 3D parametric modeler,” <https://www.freecad.org/>.
- [9] G. Kasprowicz, P. Kulik, M. Gaska, T. Przywozki, K. Pozniak, J. Jarosinski, J. W. Britton, T. Harty, C. Balance, W. Zhang, *et al.*, in *Quantum 2.0* (Optica Publishing Group, 2020) pp. QTu8B–14.
- [10] “Duke compact Ion Trap System,” <https://euriqa.pratt.duke.edu/research/compact-ion-trap-system>.
- [11] I. Pogorelov, T. Feldker, C. D. Marciniak, L. Postler, G. Jacob, O. Kriegelsteiner, V. Podlesnic, M. Meth, V. Negnevitsky, M. Stadler, *et al.*, *PRX Quantum* **2**, 020343 (2021).
- [12] R. F. Spivey, I. V. Inlek, Z. Jia, S. Crain, K. Sun, J. Kim, G. Vrijsen, C. Fang, C. Fitzgerald, S. Kross, *et al.*, *IEEE Transactions on Quantum Engineering* **3**, 1 (2021).
- [13] T. Chen, J. Kim, M. Kuzyk, J. Whitlow, S. Phiri, B. Bonduant, L. Riesebos, K. R. Brown, and J. Kim, *IEEE Transactions on Quantum Engineering* **3**, 1 (2022).
- [14] “Jayich lab ucsb double-pass-breadboard,” <https://github.com/Jayich-Lab/double-pass-breadboard>.
- [15] “Aosense rack laser system,” <https://aosense.com/products/lasers/rack-laser-system/>.
- [16] “rack-laser-system,” <https://www.aqt.eu/rowan/>.
- [17] J. Riegel, W. Mayer, and Y. van Havre, *Freecad-spec2002.pdf* (2016).
- [18] “OpenSCAD,” <https://openscad.org>.
- [19] F. Machado, N. Malpica, and S. Borromeo, *Plos one* **14**, e0225795 (2019).
- [20] “Vescent saturated absorption spectroscopy systems,” [https://www.vescent.com/manuals/doku.php?id=d2:spectroscopy\\_module\\_210](https://www.vescent.com/manuals/doku.php?id=d2:spectroscopy_module_210) ().
- [21] M. Christ, A. Kassner, R. Smol, A. Bawamia, H. Heine, W. Herr, A. Peters, M. C. Wurz, E. M. Rasel, A. Wicht, *et al.*, *CEAS Space Journal* **11**, 561 (2019).
- [22] C. Kürbis, A. Bawamia, M. Krueger, R. Smol, A. Peters, A. Wicht, and G. Tränkle, *Applied Optics* **59**, 253 (2020).
- [23] S. Madkhaly, L. Coles, C. Morley, C. Colquhoun, T. Fromhold, N. Cooper, and L. Hackermüller, *PRX Quantum* **2**, 030326 (2021).
- [24] M. Christ, C. Zimmermann, S. Neinert, B. Leykauf, K. Döringshoff, and M. Krutzik, *arXiv preprint arXiv:2402.10274* (2024).
- [25] A. Arnold, J. Wilson, and M. Boshier, *Review of Scientific Instruments* **69**, 1236 (1998).
- [26] C. Hawthorn, K. Weber, and R. E. Scholten, *Review of scientific instruments* **72**, 4477 (2001).
- [27] E. C. Cook, P. J. Martin, T. L. Brown-Heft, J. C. Gorman, and D. A. Steck, *Review of Scientific Instruments* **83** (2012).
- [28] S. Dutta, D. Elliott, and Y. P. Chen, *Applied Physics B* **106**, 629 (2012).
- [29] S. C. Doret, *Review of Scientific Instruments* **89** (2018).
- [30] E. H. Chang, J. Rivera, B. Bostwick, C. Schneider, P. Yu, E. R. Hudson, H. Collaboration, *et al.*, *Review of Scientific Instruments* **94** (2023).
- [31] V. Schkolnik, O. Fartmann, and M. Krutzik, *Laser Physics* **29**, 035802 (2019).
- [32] A. Daffurn, R. F. Offer, and A. S. Arnold, *Applied Optics* **60**, 5832 (2021).
- [33] “Thorlabs saturated absorption spectroscopy systems,” [https://www.thorlabs.com/newgrouppage9.cfm?objectgroup\\_id=5616](https://www.thorlabs.com/newgrouppage9.cfm?objectgroup_id=5616) ().
- [34] N. Akerman, *Trapped ions and free photons*, Ph.D. thesis, The Weizmann Institute of Science (Israel) (2012).
- [35] A. Madej, L. Marmet, and J. Bernard, *Applied Physics B* **67**, 229 (1998).
- [36] B. Wiegand, B. Leykauf, R. Jördens, and M. Krutzik, *Review of Scientific Instruments* **93** (2022).
- [37] K. Jung, K. Yamamoto, Y. Yamamoto, M. Miyabe, I. Wakaida, and S. Hasegawa, *Japanese Journal of Applied Physics* **56**, 062401 (2017).
- [38] T. Ruster, C. T. Schmiegelow, H. Kaufmann, C. Warschburger, F. Schmidt-Kaler, and U. G. Poschinger, *Applied Physics B* **122**, 254 (2016).
- [39] R. Ozeri, W. M. Itano, R. Blakestad, J. Britton, J. Chiverini, J. D. Jost, C. Langer, D. Leibfried, R. Reichle, S. Seidelin, *et al.*, *Physical Review A—Atomic, Molecular, and Optical Physics* **75**, 042329 (2007).

- [40] A. J. Olson, S.-J. Wang, R. J. Niffenegger, C.-H. Li, C. H. Greene, and Y. P. Chen, *Physical Review A* **90**, 013616 (2014).
- [41] C.-H. Li, C. Qu, R. J. Niffenegger, S.-J. Wang, M. He, D. B. Blasing, A. J. Olson, C. H. Greene, Y. Lyanda-Geller, Q. Zhou, *et al.*, *Nature Communications* **10**, 375 (2019).
- [42] D. Bluvstein, S. J. Evered, A. A. Geim, S. H. Li, H. Zhou, T. Manovitz, S. Ebadi, M. Cain, M. Kalinowski, D. Hangleiter, *et al.*, *Nature* **626**, 58 (2024).
- [43] H.-S. Zhong, Y.-H. Deng, J. Qin, H. Wang, M.-C. Chen, L.-C. Peng, Y.-H. Luo, D. Wu, S.-Q. Gong, H. Su, *et al.*, *Physical review letters* **127**, 180502 (2021).
- [44] N. Cooper, L. Coles, S. Everton, R. Champion, S. Madkhaly, C. Morley, W. Evans, R. Saint, P. Krüger, F. Oručević, *et al.*, arXiv preprint arXiv:1903.07708 (2019).

## SUPPLEMENTARY INFORMATION

### Design Conventions

Following some conventions (i.e. design rules) helps organize layouts, avoiding complex routing that is difficult to verify and debug.

Conventions we have found useful include:

1. **All beams at a fixed height.**
2. **All beams along a fixed 1-inch grid.** This ensures that all baseplates are compatible and easily aligned with each other. This also eases the conception of optical layout upon fixed ‘cardinal directions’.
3. **One way branching.** All baseplates branch off the same direction from the main beam (all left or all right) so all outputs into optical fibers are the same direction.

These conventions are meant to be broken for specific cases, but setting conventions aids in the modularization of larger systems.

### Adding new optical components

The component library itself is defined by a set of object classes. Each class represents a particular component and is defined by two main parts. The initialization method of the class allows you to define key parameters and arguments for part placement or design as well as defining any relevant optical properties. For example, a mirror component might have arguments for its width, height, part number, etc. as well as define the plane on which incident beams should be reflected. The second portion of the class allows you to define the modeling of the object itself as well as any drilling required for mounting. In the case of an off-the-shelf mount, this could simply be loading an STL file. However, in the case of more complex mounts or adapters, the design can be fully scripted such that the component dynamically adjusts its model using different arguments.

Ease of import and creation of new components is a crucial element of any library. As such, several systems have been put in place in an attempt to make the process as seamless as possible. For one, when scripting entirely custom component, several helper-functions have been implemented to abstract from FreeCAD’s more basic scripted geometry implementation. This includes functions to simplify the creation of basic geometries such as boxes or holes with additional options to add fillets or counter bores as required. There are also functions to help simplify the creation of drilling geometry such as a bounding box function with adjustable tolerance for recessed components.

The second major system designed for importing components is a GUI based STL import tool. A major bottleneck in importing existing mounts is properly centering the STL. Most vendors provide a model of their product in the form of STEP files, however the placement and rotation of the object in these files tends to be quite random. In order to properly use such a model with our library, it needs to be positioned at some logical origin, usually an optical center or a mounting point. For this purpose, two GUI functions were put in place in the PyOpticL workbench.

The first function allows you to orient an input STEP file and save it as an STL into the library. It works by taking a chosen STEP file and allowing the user to define an intended origin through the selection of bounding edges or points as well as define the correct orientation by rotating the view-port camera to face the front of the component. After this the generated STL is automatically exported and the required import command to be used in the object class is printed to the FreeCAD console along with all required transformations of the STEP’s positioning.

The second function is then used for measuring the offsets of additional features such as mounting holes and surfaces. This can be done in a similar fashion to how the origin is defined in the orientation function, by selecting any bounding edges or points. The function will then print to the console the position offset of that feature for use in object definitions and drill features.

### Single-pass AOM baseplate

Acoustic optical modulators (AOMs) are a core control element within most AMO apparatus, as they enable precise and fast control of laser beam intensity and frequency. Here we start with a simple design for a single-pass AOM baseplate which branches off of the main beam line from the ECDL.



Two optional input mirrors (BB05-E02, KM05) allow precise downstream alignment if necessary. Then rotation of a half waveplate (in a RSP05 mount) allows a polarizing beam splitter (PBS101) to branch off a controlled amount of optical power to the AOM. Diverted power enters the AOM (Isomet M1250-T200L-0.5) and is diffracted when RF power is pulsed through the AOM. Two mirrors allow fine adjustment of the alignment into the fiber port (PAF2-A4A), directing light through the optical fiber to the ion trap.

### Double-pass AOM baseplate

Double-pass AOM configurations are a common method for precise frequency and amplitude control over hundreds of MHz and are used in innumerable AMO experiments. Again, two optional input mirrors allow realignment of the input beam and a half waveplate allows precise control of how much power is sent into the baseplate from the PBS and how much transmits to subsequent base plates. Two input mirrors after the PBS enable independent alignment into the AOM (Isomet). Unlike a single-pass AOM configuration, a lens is placed a focal length away from the AOM so all diffracted beams are parallel to the input beam. Upon retro-reflection by a mirror, a 2nd ‘pass’ through the AOM then exactly cancels out the diffraction angle of the 1st pass so that the output laser beam counter-propagates with the original input beam, independent of the frequency sent to the AOM. This output beam now has precisely twice the frequency added from each pass through the AOM. The lens in the retro-reflection path also focuses the laser beamwaists, so the retro-reflection mirror must be placed a focal length away from the lens to ensure the output beam is collimated.

To prevent the input light from leaking into the output, an iris blocks the zeroth-order beam (and unwanted diffraction orders) just before the retro-reflection mirror, near the beam’s focus, but leaving space for a power meter probe. For our application, the rubidium transition we are locking to is 440 MHz red detuned from the strontium ion transition, so the angle of the AOM and the iris are aligned to transmit the ‘+1’ diffraction order (diffracted *away* from the RF input port). The design can also be reconfigured for the ‘-1’ order by sliding the iris toward the AOM RF input port and optimizing the AOM angle. To enable spatial separation of the counter-propagating output beam, a quarter waveplate is inserted into the retro-reflection path to rotate the input vertical polarization to horizontal so that the output beam transmits the initial PBS. Lastly, two mirrors are used to couple light into the optical fiber and to the trapped ion.

### Extended Cavity Diode Laser

Homemade extended cavity diode lasers at near-IR wavelengths were an enabling tool for pioneering AMO labs [25] which needed many narrow linewidth lasers for various atomic transitions and operations such as laser cooling and atomic state preparation and/or repumping. Not only were they completely customizable but were often an order of magnitude cheaper than commercial lasers (if commercial options existed at all). Also, the performance of these homemade ECDLs, including specifications such as linewidth and stability were often sufficient for these niche applications, which often do not require broad mode-hop-free scan ranges. However, these designs often require machining multiple custom components [22, 25–32], and are static designs for a single wavelength.

Here we focus on designing an extremely simple ECDL with only a single custom part, a dynamic 3D printed mount for the diffraction grating. All other parts are off-the-shelf from commercial vendors with no modification or machining at all. The 3D printed grating mount attaches directly to the ubiquitous KM100PM Thorlabs mount without modification. As a test case we demonstrate laser operation in the violet, specifically 421.6 nm which is useful for strontium trapped ions and also neutral rubidium for Rydberg applications. Until relatively recently, second-harmonic generation was required to achieve these wavelengths with sufficient power for various AMO applications like laser cooling.

#### *Laser Diode*

The laser diode is made by TopGaN (and Nichia) and lases directly in the violet without second harmonic generation. It is not AR coated and is mounted in 1/2 inch optics, S05LM56 and LMR05. As shown in Figure 4, the light is collimated with a C610TMD-A lens (focal length  $f=4\text{mm}$ ) mounted within a S05TM09 adapter and a 1/2 inch lens tube (SM05L05) threaded to the front of the LMR05. The LMR05 is mounted to a KM100PM which is then mounted onto a small aluminum block, which does not require any machining and can be cut to an arbitrary size by hand from

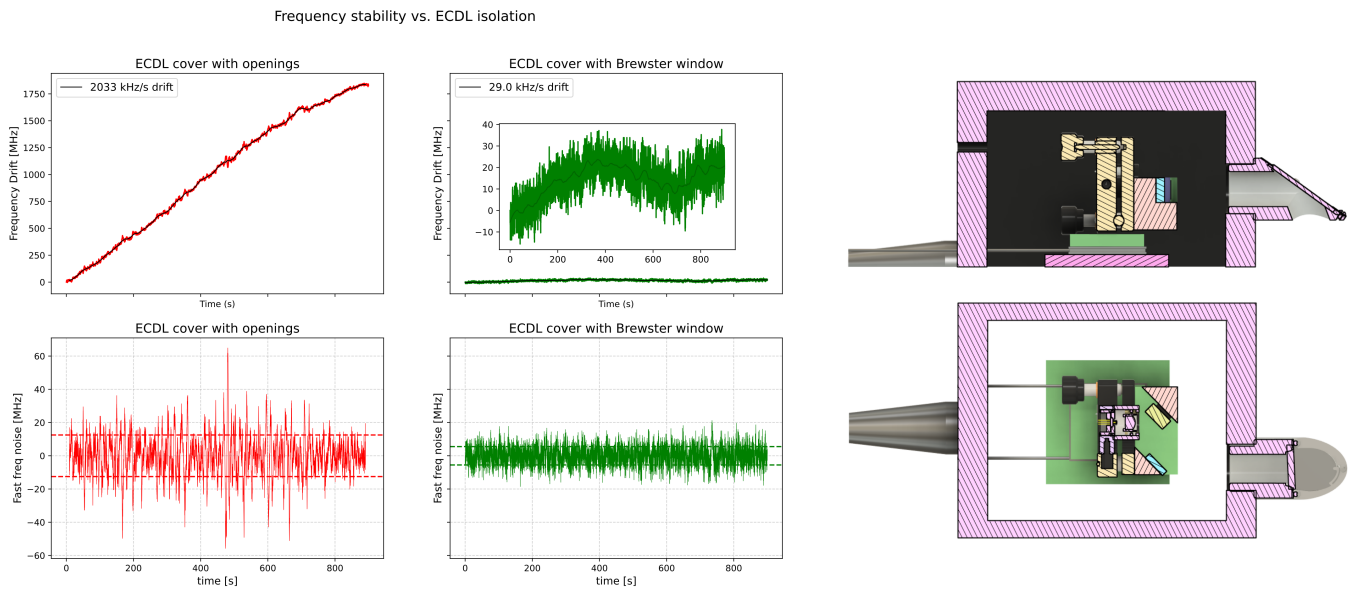


FIG. 8. **ECDL passive frequency stability:** Using a Brewster window to create a 3D printed air tight cover dramatically improves the laser stability. When the box for the ECDL has small openings for the laser, wires, and adjustment of the diffraction grating window we see drift of over 2MHz/s. When we use a Brewster window to create an air tight cover for the laser, we see this drift reduced by nearly two orders of magnitude, to 30kHz/s. Further, the fast frequency noise is reduced by half as well.

1/4 inch thick aluminum stock with a single drilled and threaded hole to mount the KM100PM. This aluminum block is epoxied to a TEC (TECH4), which is then epoxied onto a slightly larger 1/4 inch thick aluminum block (which also does not require machining). The TEC is controlled with a temperature controller (Thorlabs TED200C). Finally, the bottom plate can be mounted directly to the optical table for thermal sinking and directly match the height of the baseplates. Alternatively, the bottom plate can be placed on a sorbothane sheet for vibration isolation. The full mount is then enclosed in two 3D printed boxes for thermal isolation and stability, as well as some acoustic shielding (with additional layers improving the isolation).

#### *Dynamic grating mount*

The feedback for the extended cavity diode laser is provided by a diffraction grating (GH13-36U) mounted on a parameterized custom 3D printed mount. The Littrow angle of the grating in the mount is set within the code by inputting the wavelength and the diffraction grating pitch, allowing the design to be dynamically reconfigured for arbitrary wavelengths (and AR vs. non-AR diodes etc.). The diffraction grating is paired with a parallel mirror (ME05S-P01) to offset any angles during adjustment and mounted to the front of the KM100PM also holding the laser diode. A PZT element (PA4HKW) is placed behind the grating for precise tuning. While more sophisticated mounts are possible which only tune the angle of the grating through careful placement of the pivot point, they are not readily machined from aluminum. We anticipate the investigation of the stability of sophisticated 3D printed mounts with different materials for these applications to be an interesting direction of future research. The present design is as simple as possible to minimize machining. However, the 3D printed mount shows remarkable stability (see SI) and was used for all experiments.

#### *Temperature control*

Laser diodes are never at the exact wavelength required to address a specific atomic transition, and pre-selection of diodes to within a nanometer can easily quadruple their cost. Therefore, it is advantageous to be able to widely tune the laser diode wavelength by more than a nanometer. Coarse adjustment of the angle of the diffraction grating can broadly tune the laser diode frequency hundreds of GHz. However, tuning the temperature of the laser diode can

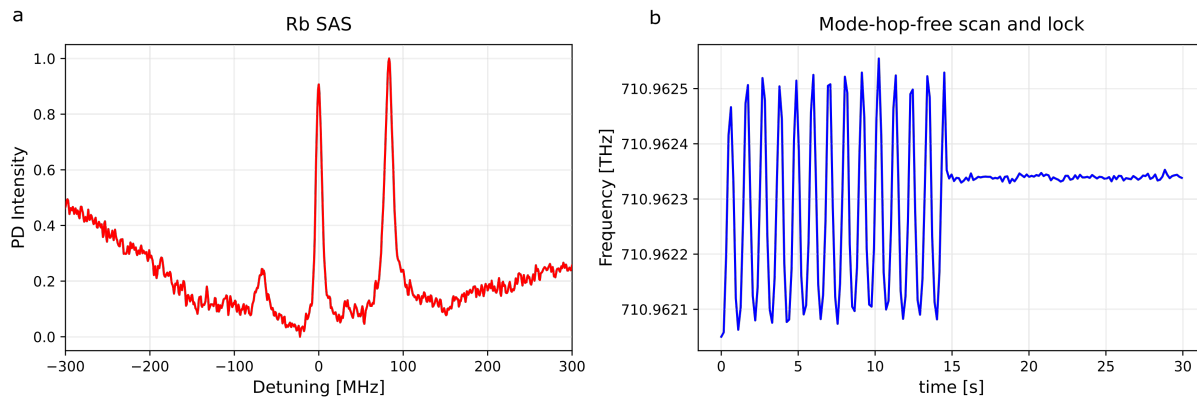


FIG. 9. **Saturated Absorption Spectroscopy:** a) Doppler free spectroscopy of the  $5s^2S_{1/2} \rightarrow 6p^2P_{1/2}$  transitions of  $^{85}\text{Rb}$  ( $F = 2 \rightarrow 2,3$ ) near 421.6 nm. b) Slowly scanning the PZT voltage shows mode-hop-free tuning over 400MHz. The laser is then locked to the center peak for absolute stabilization.

tune the frequency multiple THz, especially if the diode can be heated. Tuning via cooling is limited due to the risk of condensation, but laser diodes can often be heated more than 30 degrees, to above 50C, at the cost of decreased optical power from the increased current threshold for lasing.

We tested multiple laser diodes and in one case were able to tune a laser diode which had a free-running wavelength of 418.9 nm up to 421.6 nm (-4.6 THz) by heating the mount up to 50 C. Even at these high temperatures, the thermal stability of the laser diode was within 100MHz over the course of hours measured by a MOGLabs Fizeau wavemeter and verified with saturated absorption spectroscopy (as detailed below).

#### *Optical isolator and cylindrical telescope*

Next two mirrors are used to align the laser through an optical isolator (IO-3D-405-PBS). The efficiency of the transmission through the optical isolator is limited by the ellipticity of the laser beam, which causes clipping. Therefore, we implement a cylindrical telescope (LJ1821L1-A and LK1085L1-A) to obtain a circular beam shape. Each lens was mounted in a custom 3D printed mount. Alternatively, anamorphic prism pairs could be custom mounted within a 3D printed mount to set the required relative angle.

### **Saturated Absorption Spectroscopy**

To demonstrate stable single-mode operation of the ECDL we use it to observe saturated absorption spectroscopy (SAS). SAS is commonly used to lock and stabilize lasers using an atomic transition. We note that *many* other examples of small SAS setups exist [3, 22–24] and are commercially available [20, 33].

Here we create the entire saturated absorption spectroscopy (SAS) layout using PyOpticL (Fig. 2), and build the 1/2 inch mounted optics plate (Fig. 9b).

Similar to other baseplates, two optional input mirrors allow downstream alignment and a half waveplate allows power to be branched off with a polarizing beam splitter. A beam sampler then reflects a small amount of light to traverse the Rb cell as a ‘probe’ beam. A half-waveplate rotates the vertical polarization to horizontal so it can transmit through the final PBS and be detected by the photodiode. The rest of the optical power transmits the beam sampler as the ‘pump’ beam, with two mirrors for alignment and a PBS to allow counter propagation. The pump beam saturates the excitation of the vapor atoms at zero velocity relative to the pump for Doppler free spectroscopy. The pump power can optionally be reused by fiber coupling to a wavemeter.

The frequency was tuned by applying a high voltage (up to 150V) to the PZT and enabled mode hop free tuning over 1 GHz. Synchronous ramping with the current controller could allow broader mode hop free tuning [28]. This allowed the laser to be tuned to the resonance of rubidium and enabled capture of Doppler free peaks as shown in Figure 9a.

## Dynamic Saturated Absorption Spectroscopy Baseplate

```

1 from PyOpticL import layout, optomech
2 from datetime import datetime
3
4 name = "Rb SAS"
5 date_time = datetime.now().strftime("%m/%d/%Y")
6 label = name + " " + date_time
7
8 gap=layout.inch/8 # Offset for baseplate edges from the total size
9
10 ### Optics selection dictionary definitions
11 # Contains scaling, desired mounts, and additional parameter modifications for varying scales
12
13 # Miniature optics (2-3mm), partial inset mounting
14 mini_optics = {"scale":0.25,
15               "base_dz": layout.inch/4,
16               "optics_dz":0.5,
17               "beam_width":1.5,
18               "mirror":dict(obj_class=optomech.square_mirror, width=3, height=4, thickness=2),
19               "waveplate":dict(obj_class=optomech.waveplate, diameter=4),
20               "splitter":dict(obj_class=optomech.circular_splitter, diameter=4, thickness=2),
21               "cube_splitter":dict(obj_class=optomech.cube_splitter, cube_size=3),
22               "rb_cell":dict(obj_class=optomech.rb_cell_cube),
23               "photodiode":dict(obj_class=optomech.photodiode_fds010, x=gap)}
24
25 # Half inch optics, full inset mounting
26 half_inch_unmounted = {"scale":0.5,
27                       "base_dz":3*layout.inch/2,
28                       "optics_dz":-layout.inch/4,
29                       "beam_width":3,
30                       "mirror":dict(obj_class=optomech.circular_mirror),
31                       "waveplate":dict(obj_class=optomech.waveplate),
32                       "splitter":dict(obj_class=optomech.circular_splitter),
33                       "cube_splitter":dict(obj_class=optomech.cube_splitter),
34                       "rb_cell":dict(obj_class=optomech.rb_cell_cube),
35                       "photodiode":dict(obj_class=optomech.photodiode_fds010, x=gap)}
36
37 # Half inch optics, Thorlabs mini mounts
38 half_inch_mounted = {"scale":1,
39                    "base_dz": layout.inch,
40                    "optics_dz": layout.inch/2,
41                    "beam_width":3,
42                    "mirror":dict(obj_class=optomech.circular_mirror, mount_type=optomech.mirror_mount_km05),
43                    "waveplate":dict(obj_class=optomech.waveplate, mount_type=optomech.rotation_stage_rsp05),
44                    "splitter":dict(obj_class=optomech.circular_splitter, mount_type=optomech.splitter_mount_b05g),
45                    "cube_splitter":dict(obj_class=optomech.cube_splitter, mount_type=optomech.skate_mount),
46                    "rb_cell":dict(obj_class=optomech.rb_cell, mount_type=optomech.rb_cell_holder_old),
47                    "photodiode":dict(obj_class=optomech.photodetector_pda10a2, distance=2*layout.inch)}
48
49 # One inch optics, Thorlabs standard mounts
50 one_inch_mounted = {"scale":1.25,
51                   "base_dz": layout.inch,
52                   "optics_dz": layout.inch,
53                   "beam_width":3,
54                   "mirror":dict(obj_class=optomech.circular_mirror, diameter=layout.inch, mount_type=optomech.mirror_mount_km100),
55                   "waveplate":dict(obj_class=optomech.waveplate, diameter=layout.inch, mount_type=optomech.rotation_stage_rsp1, mount_args=dict(adapter_args=dict(mount_hole_dy=50, outer_thickness=5))),
56                   "splitter":dict(obj_class=optomech.circular_splitter, diameter=layout.inch, mount_type=optomech.splitter_mount_b1g),
57                   "cube_splitter":dict(obj_class=optomech.cube_splitter, cube_size=20, mount_type=optomech.skate_mount, mount_args=dict(mount_hole_dy=30)),
58                   "rb_cell":dict(obj_class=optomech.rb_cell, mount_type=optomech.rb_cell_holder_old),
59                   "photodiode":dict(obj_class=optomech.photodetector_pda10a2, distance=1.25*2*layout.inch)}
60
61 # Begin baseplate design
62
63

```



```

64 def Rb_SAS(x=0, y=0, angle=0, optic_type=half_inch_mounted):
65
66     # Scale baseplate size based on optics used
67     base_dx = optic_type['scale']*18*layout.inch
68     base_dy = optic_type['scale']*6*layout.inch
69
70     # Create baseplate, adjusting optical height and thickness based on desired optics
71     baseplate = layout.baseplate(base_dx, base_dy, optic_type['base_dz'], x=x, y=y, angle=angle,
72     gap=gap, optics_dz=optic_type['optics_dz'], name=name, label=label)
73
74     # Add two input beam options, for use with or without input mirrors
75     baseplate.add_beam_path(x=base_dx-optic_type['scale']*1.5*layout.inch,
76     y=0, angle=90, drill_width=optic_type['beam_width'])
77     beam = baseplate.add_beam_path(x=base_dx-optic_type['scale']*2.5*layout.inch,
78     y=0, angle=90, drill_width=optic_type['beam_width'])
79
80     # Optional input mirrors
81     baseplate.place_element_along_beam(name="input mirror 1",
82     **optic_type['mirror'], beam_obj=beam, beam_index=0b1, distance=optic_type['scale']*1.5*
83     layout.inch, angle=layout.turn['up-right'])
84     baseplate.place_element_along_beam(name="input mirror 2",
85     **optic_type['mirror'], beam_obj=beam, beam_index=0b1, distance=optic_type['scale']*1*
86     layout.inch, angle=layout.turn['right-up'])
87
88     # Add split so baseplates can be chained together
89     baseplate.place_element_along_beam(name="Half waveplate 1",
90     **optic_type['waveplate'], beam_obj=beam, beam_index=0b1, distance=optic_type['scale']*1.5*
91     layout.inch, angle=layout.cardinal['up'])
92     baseplate.place_element_along_beam(name="Beam Splitter 1",
93     **optic_type['cube_splitter'], beam_obj=beam, beam_index=0b1, distance=optic_type['scale']
94     ]*2*layout.inch, angle=layout.cardinal['up'])
95
96     # Split probe and pump beams
97     baseplate.place_element_along_beam(name="mirror 1",
98     **optic_type['mirror'], beam_obj=beam, beam_index=0b11, distance=optic_type['scale']*3.5*
99     layout.inch, angle=layout.turn['left-down'])
100
101     baseplate.place_element_along_beam(name="splitter",
102     **optic_type['splitter'], beam_obj=beam, beam_index=0b11, distance=optic_type['scale']
103     ]*0.75*layout.inch, angle=layout.turn['down-left'])
104
105     # Probe beam alignment mirrors
106     baseplate.place_element_along_beam(name="Half waveplate Probe",
107     **optic_type['waveplate'], beam_obj=beam, beam_index=0b111, distance=optic_type['scale']
108     ]*1.75*layout.inch, angle=layout.cardinal['left'])
109     baseplate.place_element_along_beam(name="probe mirror 1",
110     **optic_type['mirror'], beam_obj=beam, beam_index=0b111, distance=optic_type['scale']*1.25*
111     layout.inch, angle=layout.turn['left-down'])
112     baseplate.place_element_along_beam(name="probe mirror 2",
113     **optic_type['mirror'], beam_obj=beam, beam_index=0b111, distance=optic_type['scale']*1.5*
114     layout.inch, angle=layout.turn['down-left'])
115
116     # Rubidium Cell
117     baseplate.place_element_along_beam(name="Rb gas cell",
118     **optic_type['rb_cell'], beam_obj=beam, beam_index=0b111, distance=optic_type['scale']*3.5*
119     layout.inch, angle=layout.cardinal['right'])
120
121     # Pump beam alignment mirrors
122     baseplate.place_element_along_beam(name="pump mirror 1",
123     **optic_type['mirror'], beam_obj=beam, beam_index=0b110, distance=optic_type['scale']*3*
124     layout.inch, angle=layout.turn['down-left'])
125     baseplate.place_element_along_beam(name="Half-waveplate-pump",
126     **optic_type['waveplate'], beam_obj=beam, beam_index=0b110, distance=optic_type['scale']*4*
127     layout.inch, angle=layout.cardinal['left'])
128     baseplate.place_element_along_beam(name="pump mirror 2",
129     **optic_type['mirror'], beam_obj=beam, beam_index=0b110, distance=optic_type['scale']*5.5*
130     layout.inch, angle=layout.turn['left-up'])
131
132     # Probe beam pick-off for photodiode
133     baseplate.place_element_along_beam(name="Beam-Splitter_2",

```

```
120     **optic_type['cube_splitter'], beam_obj=beam, beam_index=0b110, distance=optic_type['scale']
121     ]*1.5*layout.inch, angle=layout.cardinal['left'])
122 # Photodiode for spectrum readout
123 baseplate.place_element_along_beam(name="Photodiode",
124     **optic_type['photodiode'], beam_obj=beam, beam_index=0b1110, angle=layout.cardinal['right']
125     ])
126
127 # Render baseplate at each of the 4 optics scales
128 if __name__ == "__main__":
129     Rb_SAS(0, 16, optic_type=one_inch_mounted)
130     Rb_SAS(0, 8, optic_type=half_inch_mounted)
131     Rb_SAS(0, 3, optic_type=half_inch_unmounted)
132     Rb_SAS(0, 0, optic_type=mini_optics)
133     layout.redraw()
```